molecules

MDPI

Article

The Use of Flavylium Salts as Dynamic Inhibitor Moieties for Human Cb_5R

Oscar H. Martínez-Costa [1,2,†], Laura Rodrigues-Miranda [1,†], Sofia M. Clemente [3], António Jorge Parola [3], Nuno Basilio [3,*] and Alejandro K. Samhan-Arias [1,2,3,*]

1 Departamento de Bioquímica, Universidad Autónoma de Madrid (UAM), C/Arturo Duperier 4, 28029 Madrid, Spain
2 Instituto de Investigaciones Biomédicas 'Alberto Sols' (CSIC-UAM), C/Arturo Duperier 4, 28029 Madrid, Spain
3 Laboratório Associado Para a Química Verde (LAQV), Rede de Química e Tecnologia (REQUIMTE), Departamento de Química, Faculdade de Ciências e Tecnologia, Universidade NOVA de Lisboa, 2829-516 Caparica, Portugal
* Correspondence: nuno.basilio@fct.unl.pt (N.B.); alejandro.samhan@uam.es (A.K.S.-A.)
† These authors contributed equally to this work.

Abstract: Cytochrome b_5 reductase (Cb_5R) is a flavoprotein that participates in the reduction of multiple biological redox partners. Co-localization of this protein with nitric oxide sources has been observed in neurons. In addition, the generation of superoxide anion radical by Cb_5R has been observed. A search for specific inhibitors of Cb_5R to understand the role of this protein in these new functions has been initiated. Previous studies have shown the ability of different flavonoids to inhibit Cb_5R. Anthocyanins are a subgroup of flavonoids responsible for most red and blue colors found in flowers and fruits. Although usually represented by the flavylium cation form, these species are only stable at rather acidic pH values (pH $\leq$ 1). At higher pH values, the flavylium cation is involved in a dynamic reaction network comprising different neutral species with the potential ability to inhibit the activities of Cb_5R. This study aims to provide insights into the molecular mechanism of interaction between flavonoids and Cb_5R using flavylium salts as dynamic inhibitors. The outcome of this study might lead to the design of improved specific enzyme inhibitors in the future.

Keywords: flavonoids; chalcones; hemiketal; flavylium; quinoidal base; cytochrome b_5 reductase

Citation: Martínez-Costa, O.H.; Rodrigues-Miranda, L.; Clemente, S.M.; Parola, A.J.; Basilio, N.; Samhan-Arias, A.K. The Use of Flavylium Salts as Dynamic Inhibitor Moieties for Human Cb_5R. *Molecules* **2023**, *28*, 123. https://doi.org/10.3390/molecules28010123

Academic Editor: H. P. Vasantha Rupasinghe

Received: 2 November 2022
Revised: 14 December 2022
Accepted: 21 December 2022
Published: 23 December 2022

1. Introduction

NADH-Cytochrome b_5 reductase (Cb_5R) is a flavoprotein that reduces multiple biological redox partners [1–7]. One of these acceptors is ferricytochrome b_5 (Cb_5), which Cb_5R reduces by using NADH in a one electron-dependent reduction reaction [8,9]. Two forms of Cb_5 have been described: a soluble and a membrane-bound form [8]. Cb_5 reduction by Cb_5R is prompted by the existence of Cb_5R isoforms co-localizing with Cb_5 isoforms [6,10].

Co-localization of this protein with nitric oxide sources has been observed in neurons [11,12]. In addition, the existence of some relatively novel redox partners in nitric oxide signaling and vascular function has been shown [13,14]. In addition, the formation of oxygen free radicals, such as superoxide anions, by reductase in the absence of electron acceptors has been described [1,10]. This radical production is stimulated in the presence of alternative electron acceptors of Cb_5, such as cytochrome *c* [15], or compounds, such as heterocyclic amines, which are potent carcinogenic agents [16]. Tight regulation of this enzyme must exist to avoid an eventual generation of both radicals (nitric oxide and superoxide anion), which production might lead to deleterious effects in cells and tissues [17]. A search for specific Cb_5R inhibitors to understand the role of this protein in this function has been initiated [13].

Flavonoids are natural polyphenols present in flowers, fruits, and other parts of some plants [18]. They are low molecular weight compounds having several beneficial

health effects, such as antioxidant, anti-inflammatory, anti-mutagenic, and anti-carcinogenic properties [18]. These substances are derived from the secondary metabolites of plants and participate in various biological functions of plants [19,20].

Flavonoids are divided into subgroups (Scheme 1), depending on the position of the B-ring and the degree of unsaturation and oxidation on the C-ring [19]. Some studies have shown that the inhibitory ability of some flavonoids, such as flavones, flavonols, flavanones, flavan-3-ols, and isoflavones, on enzymes depends on structural factors, such as double bonds between C-2 and C-3 and the presence or absence of hydroxyl groups [21,22]. The presence of two hydroxyl groups on the B ring is essential for the inhibitory effect of flavonoids on Cb_5R [22]. The inhibitory effect of these compounds decreases with increasing polarity of the groups attached to C-3, decreasing substantially when a hydroxyl group is attached in this position [21,22]. The development of new synthetic flavonoids with biological activity is important as they might help to understand the reactivity of flavonoids as possible ligands for enzymes [20].

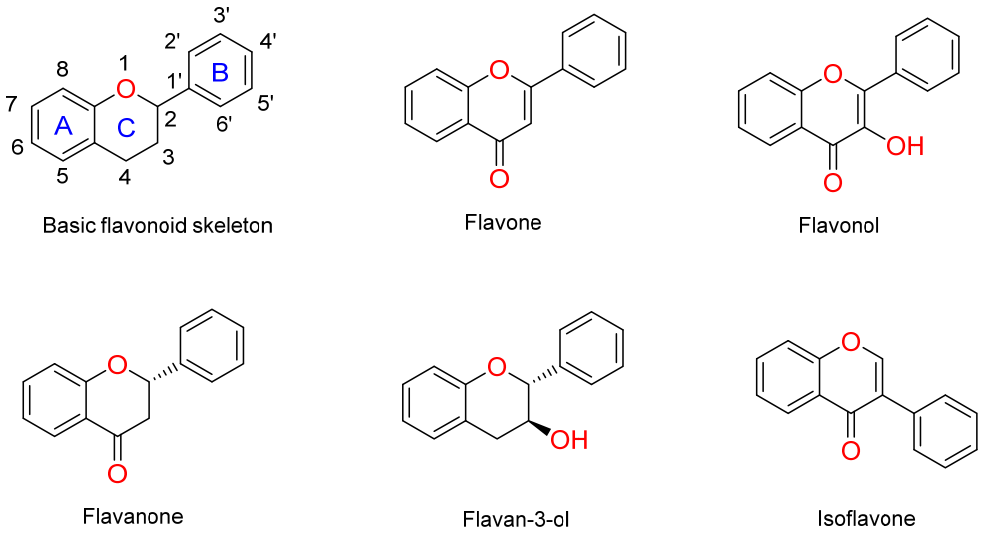

Scheme 1. Basic flavonoid structure and examples of representative flavonoid subgroups.

Anthocyanins are a subgroup of flavonoids responsible for most red and blue colors found in flowers and fruits [23]. Although usually represented by the flavylium cation form, these species are only stable at very acidic pH values leading to the reversible formation of other species at higher pH values. Scheme 2 shows the typical network of reversible chemical reactions observed for anthocyanins and synthetic flavylium salts. These dyes are usually isolated as flavylium salts. When dissolved in slightly acidic or neutral media, the red-shifted quinoidal base (A) is rapidly formed by proton transfer. However, for most compounds, these species are not the most stable, disappearing through the slower hydration of the flavylium cation to give the colorless hemiketal (B) and the *cis*-chalcone (Cc). Finally, the *cis*-chalcone may undergo a slow isomerization reaction to give the respective *trans*-chalcone (Ct). The composition of the final equilibrium strongly depends on the nature and position of the substituents decorating the flavylium core and on medium conditions such as pH, temperature, polarity, etc. This study aims to better understand the molecular mechanism of the interaction between flavonoids and Cb_5R by using flavylium salts as dynamic multistate compounds to design better inhibitors of the enzyme in the future.

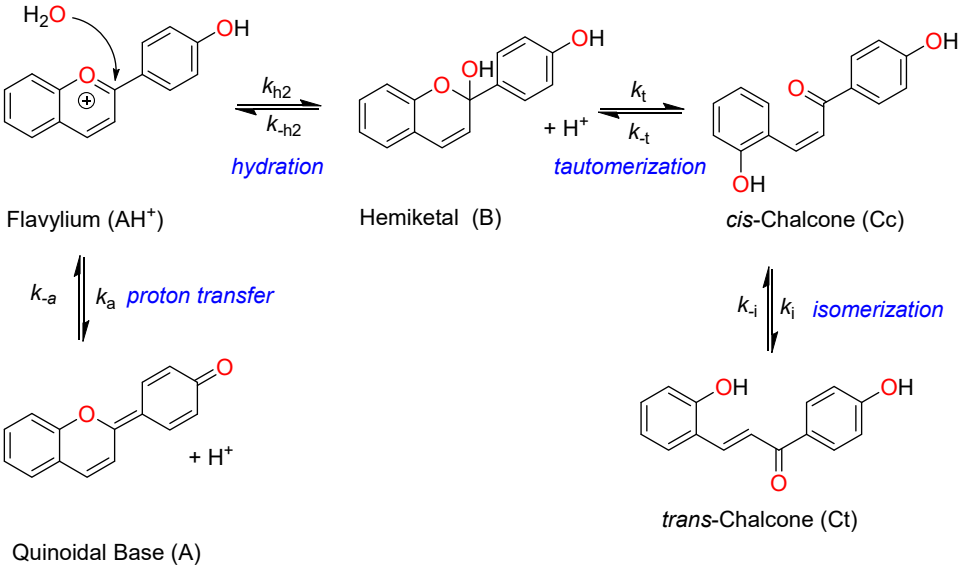

Scheme 2. General reaction network displayed by synthetic flavylium salts and anthocyanins under acidic to neutral conditions.

2. Results

2.1. Structural Interconversion of Flavylium Compounds

Five flavylium salts belonging to the anthocyanin analogs subgroup were selected for screening against the ferricyanide reductase activity of Cb_5R to study and select the most potent inhibitors based on the percentages of inhibition (Figure 1). Flavylium cations **1**, **2**, **4**, and **5** were available from previous studies [24–26]. Compound **3** was synthesized in a single step from commercially available building blocks using trimethylsilyl chloride as an acid source to generate gaseous HCl in situ.

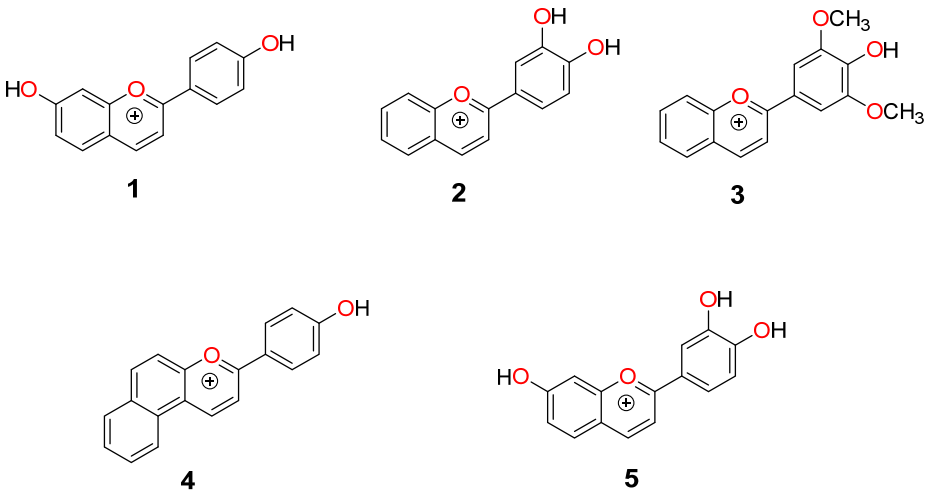

Figure 1. Chemical structures of the flavylium form of the compounds evaluated in this work as potential candidates to inhibit Cb_5R.

The stock solutions of the flavylium compounds were prepared in dimethyl sulfoxide (DMSO): H_2O (99:1) containing 0.1M of HCl. To estimate the predominant species of the used compounds (Figure 1), 10 µL of stock solution of each compound was added to potassium phosphate buffer at pH 7.0. The UV-vis spectra were recorded immediately (Figure S1, black lines) and after 2 min (red lines). No substantial spectral variations in this time scale were observed, demonstrating negligible interconversion between the species. The spectral signatures, i.e., the observation of absorption bands in the visible and UV-vis

regions, pointed out the existence of the quinoidal base and colorless hemiketal/chalcone species mixtures under non-equilibrated conditions.

2.2. *Flavylium Salts Inhibit Cb$_5$R Activities*

A pre-screening with a fixed concentration of each flavylium salt (20 μM) was performed to identify the most potent inhibitors for the ferricyanide reductase activity of C*b*$_5$R (Figure 2a). The kinetics of the ferricyanide (500 μM) reduction by C*b*$_5$R in the presence of NADH 150 μM at pH 7.0 can be compared in the absence (black squares) and the presence of compounds **1**, **2**, **3**, **4**, and **5** (labeled in red, orange, yellow, light green, and purple, respectively; Figure 2a). The activity inhibition of each compound on this activity with respect to the control (None: 340 ± 15 μmol/min/mg) was as follows: compound **1**: 36 ± 2; compound **2**: 60 ± 14; compound **3**: 143 ± 8; compound **4**: 27 ± 8; compound **5**: 5 ± 3 μmol/min/mg.

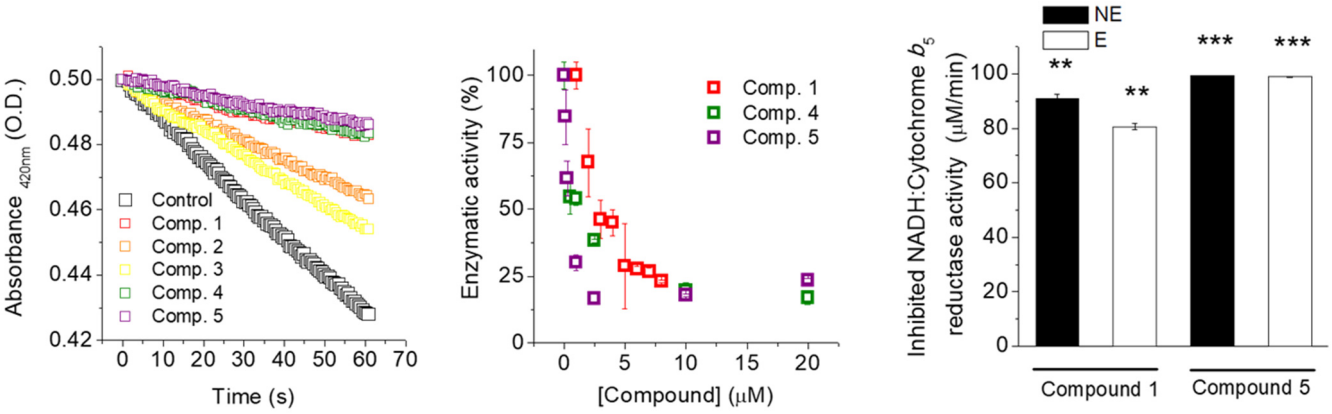

(**a**) (**b**) (**c**)

Figure 2. The inhibitory effect of flavylium salts on the reductase activities of C*b*$_5$R. The inhibitory effect of 20 μM of compound **1** (red squares), **2** (orange squares), **3** (yellow squares), **4** (light green squares), and **5** (purple squares) on the ferricyanide reductase activity of C*b*$_5$R (black squares) is shown in panel (**a**). The dependence of the ferricyanide reductase activity of C*b*$_5$R upon compounds **1**, **4**, and **5** for concentration in the calculation of these compounds' IC$_{50}$ value is shown in panel (**b**). The achieved inhibition percentages of the NADH: C*b*$_5$ reductase activity of C*b*$_5$R (0.2 μg/mL) by the non-equilibrated (NE) (black bar) and equilibrated (E) (white bar) forms of compounds **1** and **5** (20 μM) are shown in panel (**c**). Statistical significance with respect to the control (no inhibitor). ** $p < 0.01$, *** $p < 0.001$.

To further characterize the inhibitory potency of those compounds to strongly inhibit NADH: ferricyanide reductase activity of C*b*$_5$R (compounds **1**, **4**, and **5**), we calculated their IC$_{50}$ values The titration of the NADH: ferricyanide reductase with increasing concentrations of each compound is found in Figure 2b. Compounds **1**, **4**, and **5** presented the following IC$_{50}$ values of 2.14 ± 0.15 μM, 0.82± 0.019 μM, and 0.18 ± 0.03 μM, respectively (Figure 2b and Table 1).

Table 1. Summary of the calculated achieved inhibition at 20 μM concentration and IC50 values for the non-equilibrated species of compounds tested in Figure 1B.

Compound	IC$_{50}$ (μM)	Maximum Inhibition (%)
1	2.14 ± 0.15	78 ± 1
4	0.82 ± 0.19	85 ± 3
5	0.18 ± 0.03	93 ± 1

Compounds **1** and **5** were selected to investigate the dependence of the IC_{50} value with their respective quinoidal base or *trans*-chalcone species. Stock solutions of compounds at acid pH values (non-equilibrated (NE) in the media) and by incubation in phosphate buffer at pH 7.0 for 24 h were prepared, and their UV-vis was measured in phosphate buffer pH 7.0. As expected, the mole fraction of the quinoidal base of compounds **1** and **5** partially disappeared, leading to the formation of the respective *trans*-chalcone species after a 24 h incubation in phosphate buffer at pH 7.0 (Supplementary Figure S2). We monitored the spectra of compounds **1** and **5** (black and grey line, respectively) after immediate addition into phosphate buffer pH 7.0 (continuous line) or after incubation in this buffer for 24 h (dotted line). Our data indicate that ca. 40% of the quinoidal base (relative to its value after a 2 min incubation, λ_{max} > 500 nm) disappeared, forming the *trans*-chalcone (λ_{max} ~ 380 nm) after incubating the molecules in phosphate buffer for 24 h.

The variation of the IC_{50} value for the NE and E forms compounds **1** and **5** against the NADH: ferricyanide reductase activity of Cb_5R is shown in Table 2. The calculated IC_{50} values for the NE solutions of compounds **1** and **5** were: 2.14 ± 0.15 and 0.18 ± 0.03 μM, and for the E forms: 4.25 ± 0.83 μM and 2.12 ± 0.50 μM, respectively (Table 2). Our results indicate that the inhibitory properties of these compounds, including the IC_{50} values, might shift depending on the predominant species present in the solution, suggesting that the quinoidal base species are the species inhibiting the enzyme or they are more potent inhibitors of the reductase than the *trans*-chalcone species.

Table 2. Summary of calculated IC50 for the equilibrated and non-equilibrated forms of compounds **1** and **5**.

Compound	IC_{50} (μM)	
	Equilibrated	**Non-Equilibrated**
1	4.31 ± 0.83	2.14 ± 0.15
5	2.14 ± 0.50	0.18 ± 0.03

Cb_5 is the endogenous natural substrate of Cb_5R in biological samples. To further assess and compare the inhibitory properties of compounds **1** and **5** in non-equilibrated (NE) and equilibrated (E) conditions, we measured their effect on the NADH: Cb_5 reductase activity of Cb_5R (Figure 2c) at 20 μM concentration, in the presence of human soluble Cb_5 (5 μM), purified human soluble Cb_5R reductase (0.2 μg/mL) and NADH (150 μM). The NE forms of compounds **1** and **5** achieved an activity inhibition of 90.9 ± 1.5% and 99.3 ± 0.1%, respectively (Figure 2c), while the E forms of compounds **1** and **5** achieved 73.2 ± 1.2% and 98.9 ± 0.1%, respectively.

2.3. Type of Inhibition of the NADH: Ferricyanide Reductase Activity

We determined the inhibitory mechanism of compounds **1** and **5** against the NADH: ferricyanide reductase activity of Cb_5R (0.35 μg/mL) by titrating this activity against the NADH concentration in the presence of compound **5** (NE). As shown in Figure 3a, the measured V_{max} for this activity was 95 ± 9 μM/min (open squares), which decreased in a concentration-dependent manner to 74 ± 2 and 53 ± 1 μM/min, in the presence of 0.015 μM (open circles) and 0.03 μM (open triangles) of compound **5**, respectively. To better shed light on the type of inhibition, we performed a Lineweaver-Burk data analysis (Figure 3b). A similar K_m value was obtained from the performed measurements in the absence and presence of the NE species of compound **5**: 26 ± 1 μM of NADH and different *V*max values as reported by line fitting of the data (red line) cutting at the *x*-axis and the *y*-axis, respectively. This result suggests that the NE species of compound **5** act as a non-competitive inhibitor of the NADH: ferricyanide reductase of Cb_5R. In addition, based on our data, the calculated inhibition constant value (K_i) for the NE species of compound **5** was 0.04 μM.

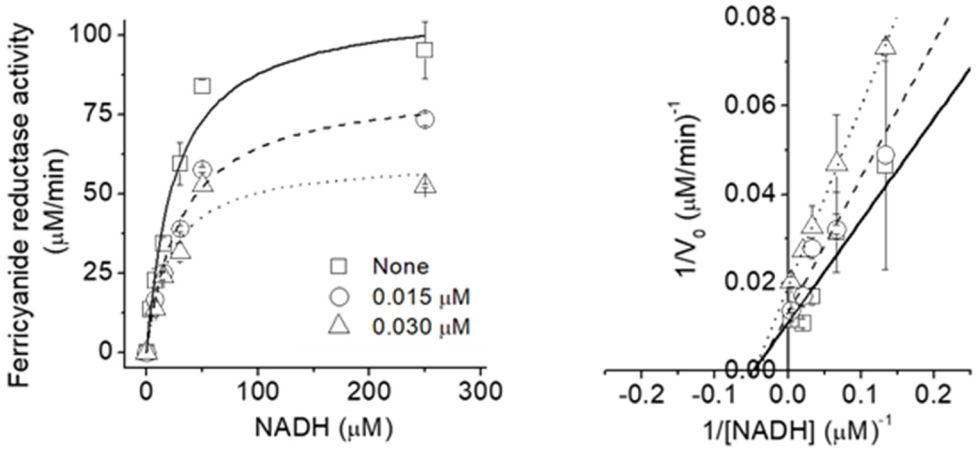

(**a**) (**b**)

Figure 3. Measurement of kinetic parameters and model for the complex formation between the NE form compound **5** and Cb_5R. The dependence of the NADH: ferricyanide reductase activity of Cb_5R reductase (0.2 μg/mL) upon NADH concentration, in the absence (open squares) and presence of constant concentrations of E forms of compound **5** (0.015 μM and 0.030 μM, open circles and open triangles, respectively) is shown in panel a. The Lineweaver–Burk representation of the data plotted in panel (**a**) is shown in panel (**b**).

*2.4. Determination of the Dissociation Constant of the Non-Equilibrated and Equilibrated Forms of Compounds **1** and **5** to Cb_5R*

Analysis of the dissociation constant of the NE and E forms of compounds **1** and **5** for the complex formation with the reductase was determined by tracking the changes in the intensity of the Cb_5R FAD's autofluorescence (Figure 4), as previously performed for other ligands of the reductase [7].

Data fitting allowed us to measure a dissociation constant of 31.2 ± 4.7 nM and 28.0 ± 2.2 nM, for the respective NE and E forms of compound 1 and 29.2 ± 5.0 nM and 19.1 ± 1.5 nM, for the respective NE and E forms of compound 5.

*2.5. Molecular Docking for the Creation of In Silico Models for the Complex Formation between the Quinoidal Base (A) and trans-Chalcone (Ct) of Compounds **1** and **5** with Cb_5R*

Using Autodock Vina [27], we created and selected a model for the complex formation between Cb_5R (PDB:1I7P) and the quinoidal base (A) and *trans*-chalcone (Ct) species of compounds **1** and **5**. The interacting site for each compound was defined as the amino acid residues that contacted the previously indicated species with a spacing of 0.35 Å and radii of 0.06 Å using AutodockTools 1.5.6 [28].

Amino acid residues of the reductase that contacted the A and Ct species of compounds **1** and **5** are shown in Table 3. Gly179 and Pro275 side chains contact with A and Ct of both compounds (Table 3 and Figure 5a,b, blue labeled). Met278 and Phe251 side chains were found to contact the A form of compound **1** (Table 3 and Figure 5a,b, red labeled). In addition, Met278 and Phe251 side chains were found to contact the A and Ct species of 5 (Table 3 and Figure 5a,b, red labeled). One amino acid side chain (Ala282) was found to contact the A species of compound **1** (Table 3 and Figure 5a,b, yellow labeled). Two amino acid side chains (Tyr 112 and Gln210) were found to contact the Ct species of compound **5** (Table 3 and Figure 5a,b, green-labeled). We also found the formation of an H-bond between the imine group (HN1 atom) of the glutamine 210 residue, involved in the peptide bond, with the hydrogen atom of the hydroxide group located in carbon four of the trans-chalcone species of compound **1**. Sequence alignment of rat PDB structure 1I7P linear sequence with the sequence of human Cb_5R showed no differences between isoforms concerning residues forming these isoforms (Supplementary Figure S3).

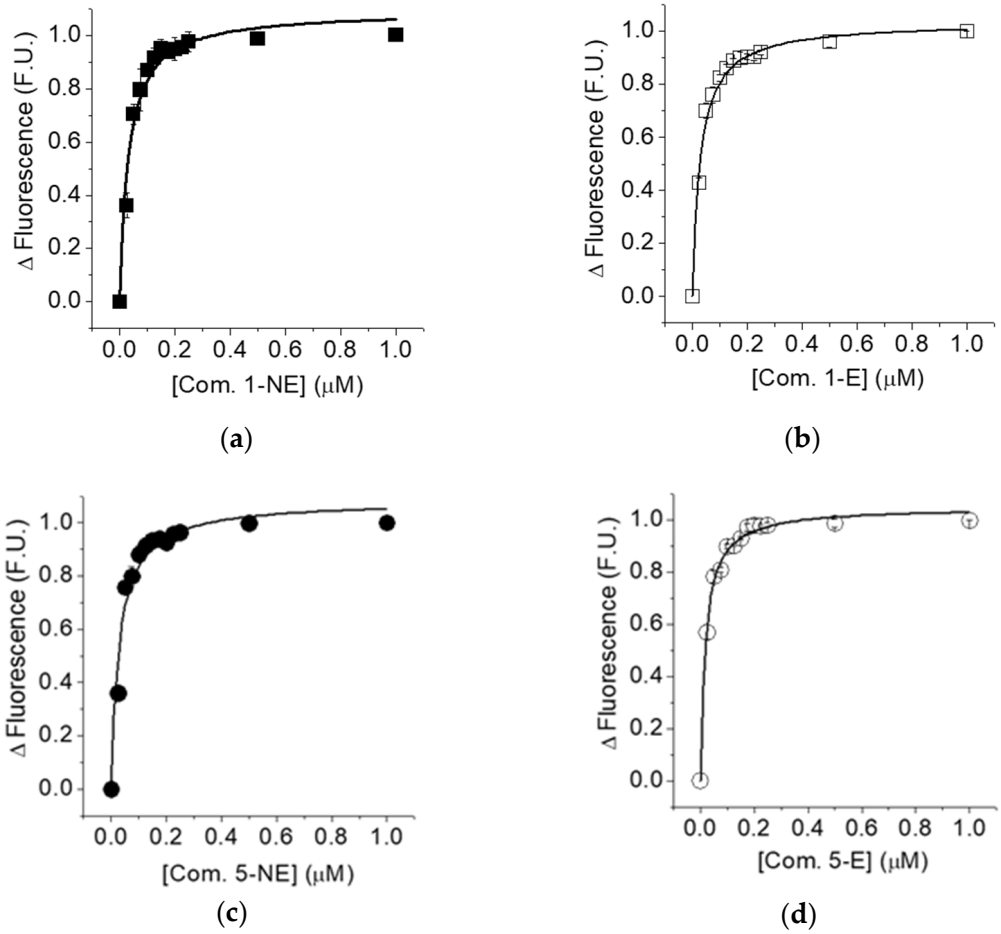

Figure 4. The dependence of Cb_5R's autofluorescence increase upon the concentration of the NE and E form of compound **1** (panels (**a**,**b**)) and the respective forms of compound **5** (panels (**c**,**d**)) let us calculate the dissociation constant as reported in the Material and Methods section.

Table 3. Summary of docking analysis for the complex formation between the quinoidal base (A) and trans-chalcone (Ct) forms of compounds **1** and **5**.

	Ligand	Affinity (kcal/mol)	Residues from the Receptor That Contact the Ligand
Cb_5R	Compound 1-A	−7.5	**Gly179**, Ala203, **Pro275**, **Met278**, **Phe251**, **Ala282**
	Compound 1-Ct	−7.2	**Tyr112**, **Gly179**, Thr181, Gly182, **Gln210**, Asp214, Gly274, **Pro275**
	Compound 5-A	−7.5	Asn209, **Phe251**, **Pro275**, Pro277, **Met278**, Phe 281, **Ala282**
	Compound 5-Ct	−7.3	**Tyr112**, Gly180, Ala208, Asn209, **Gln210**, Thr237, **Phe251**, Val252, **Pro275**, **Met278**

*2.6. Compounds **1** and **5** Inhibit NADH-Dependent Activities of the Cb_5R in Microsomes*

To further assess the biological relevance of the tested compounds as inhibitors of the Cb_5R, we measure the inhibition dependence of the NADH: ferricyanide reductase activity in rat liver microsomes (Figure 6a). All tested compounds follow a dose-dependent effect on this activity, although the maximum inhibition achieved for them was not the same as measured with the purified recombinant enzyme. The E forms of compound **5** achieved a maximum inhibition of 81 ± 2%, while the NE forms achieved a 77 ± 2% up to a compound concentration of 100 μM. An 85 ± 2% inhibition was found for the E forms of compound **1**, while the NE forms of compound **1** non-significative inhibited 11 ± 7% of the NADH: ferricyanide reductase activity. We also determined the IC_{50} values for each compound against the NADH: ferricyanide reductase activity of microsomes (5.6 μg/mL of protein) to

obtain the following values: ND, 18.0 ± 3.8 μM, 8.0 ± 2.2 μM, and 3.3 ± 0.4 μM. for the NE and E forms of compound **1** and the NE and E forms of compound **5**, respectively.

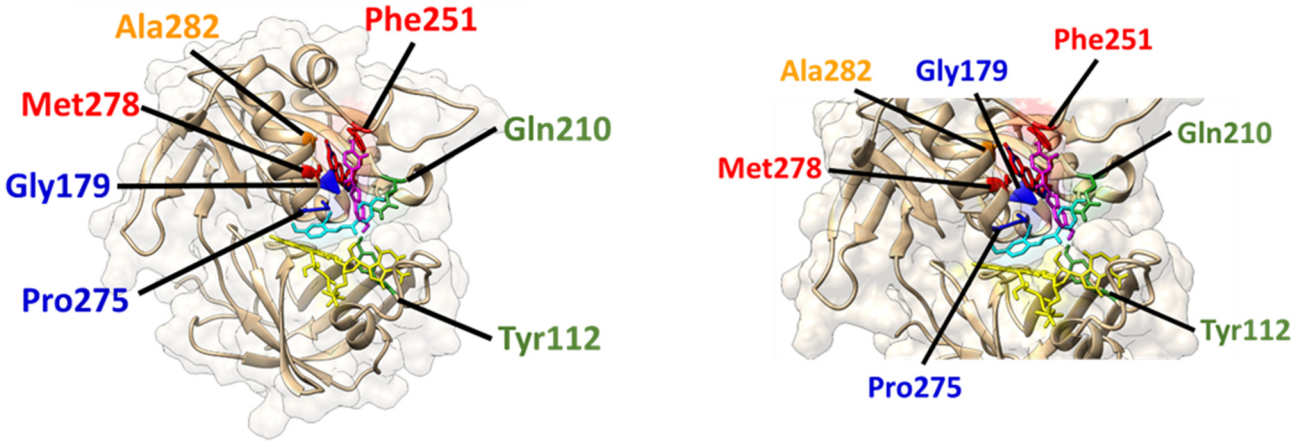

(a) **(b)**

Figure 5. Model for the complex formation between the quinoidal base (A) and *trans*-chalcone (Ct) forms of compound **1** (A and Ct forms are labeled in dark and light blue, respectively) and **5** (A and Ct are labeled in red and pink, respectively) and Cb_5R (light brown backbone) is shown in panel (**a**). The flavin group is labeled in yellow, and the location of amino acid residues that contact the ligands are labeled with the following color code: Tyr112 (olive), Gly179 (blue), Gln210 (olive), Phe251 (red), Pro275 (blue), Met278 (red), Ala282 (orange). A surface representation of the previously indicated amino acid side chains contacting the ligands is shown in panel (**b**).

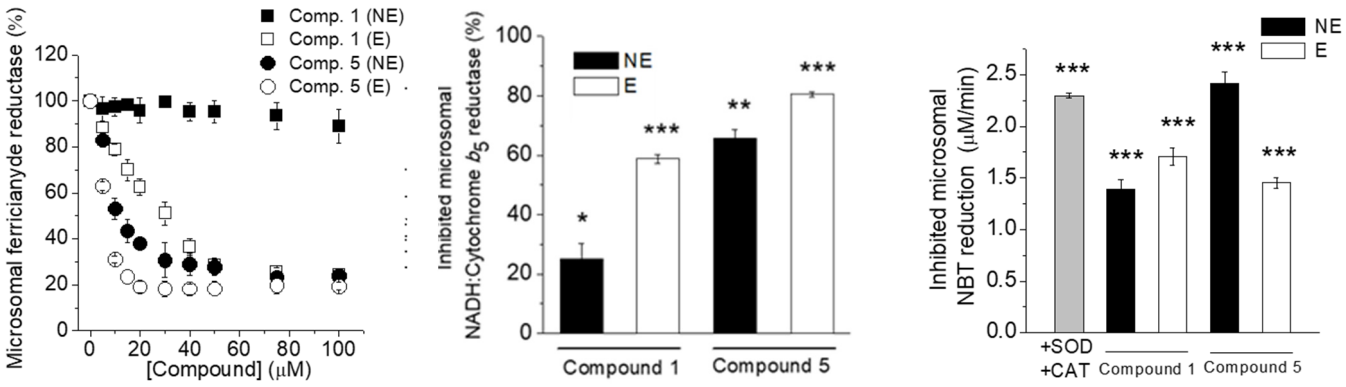

(**a**) (**b**) (**c**)

Figure 6. Inhibitory effect of the NE and E forms of compounds **1** and **5** on the NADH-dependent activities of the Cb_5R in microsomes at pH 7.0. The NADH: ferricyanide reductase activity of microsomes (11.2 μg/mL) was measured in the presence of NADH (150 μM), ferricyanide (500 μM), and at increasing concentrations of the NE and E forms of compound **1** and **5** was measured at a 420 nm fixed wavelength (panel (**a**)). The NADH: ferricytochrome b_5 reductase activity of microsomes (11.2 μg/mL) was measured in the presence of NADH (150 μM), Cb_5 (5 μM), and a fixed concentration of NE and E forms of compound **1** and **5** (40 μM) at 557 nm wavelength (panel (**b**)). Inhibition of the NADH: NBT reductase activity of microsomes by the presence of SOD (5 U/mL) + CAT (2 U/mL) (grey bar) or by the presence of the NE or E forms of compound **1** (black bar and white bar, respectively) and **5** (black bar and white bar, respectively) as shown in panel (**c**). Statistical significance with respect to the control (no inhibitor or in the absence of +SOD + CAT). * $p < 0.05$, ** $p < 0.01$, *** $p < 0.001$.

Since in biological membranes, enzymatic activities alternative to Cb_5R exist using ferricyanide as a substrate, we further assessed the inhibitory effect of compounds **1** and **5**

in the reductase activity of the Cb_5R using Cb_5, as a natural and more specific substrate of the Cb_5R, in the presence of NADH. We measured the inhibition of the NADH: Cb_5 reductase activity with a fixed concentration of the compounds (Figure 6b) and compared the values with those of the NADH: ferricyanide reductase activity in microsomes (Figure 6a). In the presence of Cb_5, the NE and E forms of compound **1** (40 μM) inhibited this activity by 25.0 ± 5.3% and 58.8 ± 1.5%, respectively; and for the NE and E forms of compound **5** by 65.6 ± 2.9 and 80.6 ± 0.8%, respectively. The inhibition of the NADH: ferricyanide reductase activity of microsomes using the same concentration of each of the tested compounds: 4.6 ± 4%, 63.4 ± 3.6% for the NE and E form of compound **1**, and 71.0 ± 4.7% and 81.8 ± 2.3% for the NE and E form of the compound **5**, correlated with those of the NADH: Cb_5 reductase activity.

Finally, we measured the effect of compounds **1** and **5** on the previously described NADH-dependent superoxide anion production of the Cb_5R by quantifying the inhibitory effect of the compounds on the NADH: nitro blue tetrazolium (NBT) reductase activity of Cb_5R from microsomes sensitive to superoxide dismutase (SOD) and catalase (CAT) (Figure 6c). The NADH: NBT reductase activity of Cb_5R measured with microsomes (5.2 μg/mL) was 4.4 ± 0.1 μM/min. Quantification of the inhibition of the NADH: NBT reductase activity of microsomes sensitive to SOD and CAT allowed us to measure a superoxide anion production by the rat microsomes of 2.3 ± 0.1 μM/min (52.2% of the total activity). The superoxide anion production dropped to 1.7 ± 0.1 and 1.4 ± 0.1 μM/min for the non-equilibrated and equilibrated forms of compound **1** and to 1.4 ± 0.1 and 2.4 ± 0.1 μM/min for the NE and E forms of the compound **5**, respectively.

3. Discussion

Cb_5R is an enzyme that participates in liver drug detoxification, mainly within microsomal membranes [5]. We have also described that Cb_5R is the main component of the plasma membrane NADH: oxidase activity of neurons that has been implicated in the NADH-dependent superoxide anion production in neuronal apoptosis [10,15,29]. The activity of the enzyme is modulable by Cb_5 levels as a natural ligand of the Cb_5R, and the superoxide anion production can be stimulated by Cb_5R complexation with cytochrome *c* and other substrates, although this enzyme can also induce superoxide anion radical production in the absence of other electron acceptors rather than oxygen [1,6,15].

Flavonoids are a family of natural polyphenols with antioxidant properties and potential use as a pharmacological drug for treating diseases, including neurodegenerative diseases [18,19]. Some flavonoids can inhibit the plasma membrane NADH oxidase of neurons blocking the associated superoxide anion production of cerebellar granular cells undergoing apoptosis in culture and the observed oxidative stress in rat models of neuropathies [30–32]. In addition, some flavonoids are inhibitors of the NADH: Cb_5 reductase and NADH: ferricyanide reductase of Cb_5R [22], which suggests that part of the superoxide anion production described to be produced in animal models of neuropathies and blocked by flavonoids could be ascribed to the production by this reductase [30–32]. On the other hand, flavylium salts which comprise anthocyanins dyes belonging to the flavonoid family, display a complex network of interconverting chemical species that can be modulated by the pH of the media [20,23]. In this work, we selected a group of synthetic flavylium salts based on the previous description of the inhibitory profile of flavonoids as inhibitors of Cb_5R to shed light on the fact that the flavonoid inhibitory behavior can be dependent on the predominant flavylium species present in solution, which mole fraction distribution can be modulable by medium conditions and external stimuli.

A prescreening of the inhibitory effect on the NADH: ferricyanide reductase activity of Cb_5R that was later assessed with the NADH: Cb_5 reductase activity of the protein allowed us to select two main inhibitors based on the low IC_{50}, the compound **1** and **5**. We determined that both the NE and E-species of these compounds could inhibit the reductase, although the NE forms were more effective in terms of lower IC_{50} for the inhibition. In these terms, the effect of compound **5** should be emphasized. Interestingly, besides the difference

found in terms of IC_{50} between compounds **1** and **5**, which is more than one order of magnitude between the NE forms (2.14 ± 0.15 μM and 0.18 ± 0.03 μM for compounds **1** and **5**, respectively), the calculated dissociation constant for all the tested compounds was, in the low nanomolar range (≈15–25 nM).

Two compounds, **1** and **5**, present a certain degree of homology by the presence of one hydroxyl group at carbon position seven of the A-ring and one or two hydroxyl groups at carbon three and four of the B-ring, respectively. The presence of these hydroxyl groups at these positions in compounds **1** and **5** contrast with their relatively high inhibition of NADH: ferricyanide activity of Cb_5R with respect to other flavylium salts. For this reason and by comparison, it might be proposed that the presence of two hydroxyl groups at carbon position seven of the A-ring and four of the B-ring are key for inhibiting Cb_5R. In addition, one additional hydroxyl group at carbon three of the B-ring seems to increase the inhibitory properties. Compound **4** also presented a relatively high inhibition of the NADH: ferricyanide activity of Cb_5R but no described flavonoids with similar minimal structural homology has been tested up to our knowledge.

Molecules with the same characteristics in the group of flavonoids used as inhibitors of Cb_5R were not found [22]. Noteworthy, flavonoids presenting a hydroxyl group at carbon four of the B-ring and at least the hydroxyl group at carbon seven of the A-ring are inhibitors of Cb_5R activity: Naringenin did not inhibit Cb_5R as shown by in vitro studies. An IC_{50} of 36 μM for apigenin against NADH: ferricytochrome b_5 reductase was found. Flavonoids presenting an additional hydroxyl group at de carbon four of the B-ring show higher inhibitory properties such as luteolin, quercetin, catechin, epicatechin, and taxifolin with $IC_{50'}$s of 0.11 μM, 1.1 μM, 4.5 μM, 3.2 μM, N.D. [22]. This extra hydroxyl group is present in our compound 5 that have a lower IC_{50} value (IC_{50} 0.18 ± 0.03 μM) concerning compound **1** (IC_{50} 2.14 ± 0.15 μM), does not have a hydroxyl group at de carbon three of the B-ring. Our data suggest that compound **5** in the non-equilibrated form is at least as efficient as the flavonoid luteolin as an inhibitor of Cb_5R.

By a competitive assay against NADH, as the natural electron donor of the reductase, we determined that the inhibition mechanism of the NE form of compound **5** was non-competitive. Docking analysis against the structural model of the reductase confirmed this point since, in comparison to NADH, the tested compounds exhibited different interacting sites [1]. The analysis of the interaction between Cb_5R's residues with compounds highlights the presence of Gly179 and Pro275 in both the A and Ct species of compound **1**. Met278 and Phe251 residues were present in both the A and Ct species of compound **5**. When the analysis is made in relationship with residues that contact the A or the Ct species, we found that Met278, Phe251, and Ala282 were present in the A species of compounds **1** and **5**, while Gln210 was present in the Ct species of compound **1** and **5**. Finally, we assessed the biological relevance of our findings by testing the action of compounds **1** and **5** against the Cb_5R present in rat liver microsomes. The weak inhibition found for the NE form of compound **1** against the NADH: ferricyanide reductase, later confirmed by the measurement of the NADH: Cb_5 reductase of microsomes, contrasted with the inhibitory profile of E species of compound **1** and the same behavior of the NE and E species of compound **5**. We attributed this result to the higher hydropathy index of the NE species rather than the E ones.

On the other side, it was confirmed that the tested compounds inhibited the NADH-dependent superoxide anion production of microsomes. The most potent inhibitory compound was the E form of compound **5** which blocked the superoxide anion production of the membranes at similar levels to those raised by the presence of SOD/CAT in the assay (2.3 ± 0.1 μM/min by 5.2 μg/mL of microsomes).

We conclude that flavylium salts can constitute interesting flexible tools for developing inhibitors against the Cb_5R that can be modulable by medium conditions and external stimuli due to their multistate properties. This family of compounds opens the door to developing modified molecules with higher specificity and susceptible to being activated

under pH-dependent variables such as acid organelles or conditions such as cellular acidosis as that observed in many pathological conditions.

4. Materials and Methods

4.1. Reagents

All reagents used in this work were of maximum grade from Sigma-Aldrich or Merck.

4.2. Synthesis

Flavylium salt **3** was synthesized as described by Al Bittar et al. for other flavylium salts [33]: salicylaldehyde (62 mg, 0.51 mmol) and 4′-4ydroxy-3′,5′-dimethoxy acetophenone (100 mg, 0.51 mmol) were dissolved in a 3 mL of ethyl acetate: methanol (2:1, *v:v*). After carefully adding 20 equivalents of trimethylsilyl chloride at room temperature, a dark red solid begins to precipitate. After stirring overnight, the solid was separated by centrifugation and thoroughly washed with ethyl acetate and diethyl ether to give the chloride salt of flavylium as a dark red powder in quantitative yield (160 mg). ^{1}H NMR (400 MHz, Methanol-d4 acidified with DCl) δ 9.18 (d, J = 9.2 Hz, 1H), 8.80 (d, J = 9.2 Hz, 1H), 8.34 (d, J = 8.6 Hz, 1H), 8.26–8.19 (m, 2H), 7.95–7.85 (m, 3H), 4.07 (s, 6H). ^{13}C NMR (101 MHz, MeOD) δ 175.85, 156.86, 154.12, 150.72, 150.37, 139.17, 131.43, 130.67, 124.97, 120.08, 120.04, 118.86, 110.29, 57.56. HRMS-ESI (positive mode) m/z calculated for ($C_{17}H_{15}O_4^+$) [M–Cl^-]: 283.0965; found, 283.0963.

4.3. Purification of Cb_5R and Cb_5

Purification of the soluble isoform of Cb_5R and the human erythrocyte isoform of Cb_5 was performed as indicated previously shown [7,15].

4.4. Microsome Preparation from Rat Liver

Livers were obtained from add livitum rats. Microsomes were prepared as previously performed, with slight differences [1]. After livers extraction, they were washed and rinsed three times in 10 mM Tris-CL, 0.25 M sucrose, 1 mM EDTA, and 1 mM phenyl sulfonyl fluoride (PMSF) at a pH value of 8.1; livers were chopped and homogenized using a PYREX® Potter-Elvehjem Tissue Grinder with PTFE Pestle. Buffer (3 mL) was used per gram of liver tissue. After homogenization, the lysate was centrifuged at 960× *g* for 10 min at 4 °C. The supernatant was collected and centrifuged at 9800× *g* for 20 min at 4 °C. Finally, the supernatant was centrifuged at 53,170× *g* for 60 min at 4 °C. The microsomal sediment was resuspended in the same buffer and frizzed at −80 °C until use.

4.5. Protein Determination

Protein was determined by Bradford [34].

4.6. Preparation of the Non-Equilibrated and EQUILIBRATED Forms of the Flavylium Cations

The transition between the acid or non-equilibrated and the equilibrated form of the flavylium salts is slow. It occurs after incubation at the determined pH in our used conditions and buffers for days. This fact allowed us to measure the effectiveness of the compounds at pH 7.0 without structural shift at times used to measure the enzymatic activities at pH 7.0.

The salts were dissolved In acidified DMSO with 0.1M of HCl to obtain the non-equilibrated or acid form of the compounds. The equilibrated or chalcone forms of the compounds were obtained by incubation in phosphate buffer pH 7.0 for 48 h.

4.7. Measurement of the Activities of the Cb_5R

The NADH: ferricyanide reductase activity was measured at room temperature in 20 mM de phosphate buffer (pH 7.0), 0.15 mM NADH, 0.5 mM ferricyanide, and Cb_5R (0.2 μg/mL) or microsomes (5.6 or 11.2 μg/mL), in the absence or presence of the flavylium salts, using a 10 mm quartz cuvette and a spectrophotometer (Perkin Elmer Lambda40,

Perkin-Elmer, Foster City, CA, USA) with a fixed wavelength at 420 nm, for the times indicated in the figures. An extinction coefficient of ferricyanide of 1 mM^{-1} cm^{-1} [1,2,6] was used to calculate the enzymatic rates.

For the NADH: Cb_5 reductase activity of Cb_5R, the following buffer was used: 20 mM de phosphate buffer (pH 7.0), 0.15 mM NADH, 5 μM of Cb_5 and 0.2 μg/mL ug/mL of Cb_5R or 5 μg/mL microsomes, in the absence or presence of the flavylium salts, using a 10 mm quartz cuvette and a spectrophotometer. A differential extinction coefficient for the Cb_5 reduction at 557 nm of 16.5 mM^{-1} cm^{-1} was used to calculate the enzymatic rates.

For the superoxide anion production, the NADH: NBT reductase activity of Cb_5R sensitive to SOD (5.2 mU/μL) and CAT (4 μg/mL) was measured in the following buffer: 20 mM de phosphate buffer (pH 7.0), 0.15 mM NADH, 0.1 mM of NBT and 0.2 μg/mL of Cb_5R or 5 μg/mL microsomes, in the absence or presence of the flavylium salts, using a 10 mm quartz cuvette and a spectrophotometer. A differential extinction coefficient for the Cb_5 reduction at 560 nm of 27.8 mM^{-1} cm^{-1} was used to calculate the enzymatic rates when needed [15].

4.8. Determination of the Dissociation Constants for the Complex Formation between the Human Recombinant Cb$_5$R and the Flavylium Salts

Determination of the dissociation constant for the complex formation between the different forms of the compound **1** and **5** was achieved by analyzing the change of the intrinsic autofluorescence of the flavin group of the reductase after complex formation, as previously used for other ligands of the reductase [6,7]. The fluorescence intensity of the Cb_5R after the sequential addition of increasing amounts of compound to phosphate buffer saline buffer (PBS) in the presence of Cb_5R (0.25 μM) while stirring at pH 7.0 at 25 °C was monitored using a spectrofluorometer (Photon Technology International Inc., Quantamaster, Ford, UK) and fixed excitation and emission wavelength at 470 and 520 nm and using a 2 mL quartz cuvette. The obtained data after titration were adjusted to the following equation for the calculation of the K_d for the complex formation:

$$F - F_0 = ([\text{Compound}] \times F_{max})/(K_d + [\text{Compound}])$$

where F is the Cb_5R fluorescence change induced by the addition of the compounds to the cuvette, F_0 is the initial Cb_5R fluorescence and F_{max} is the fluorescence increment after adding the compounds, and K_d is the dissociation constant value.

4.9. Molecular Docking Analysis

AutodockTools was used to prepare the pdbqt files based on the obtained file for the Cb_5R from the Protein data bank with the code PDB code 1I7P de Protein Data Bank (PDB) that corresponds to that obtained by X-Ray diffraction of the crystal structure of the rat Cb_5R in complex with FAD [35]. The files for the structure of the flavylium salts were prepared with the software Chemdraw 20.0 (PerkinElmer). The molecular docking analysis to study the interaction between Cb_5R (receptor) and the flavylium salts (ligands) was performed with Autodock Vina [27]. From all the possible conformation and clusters, the highest affinity was selected with the higher number of poses as the model for the complex formation. The interacting site for each compound was defined as the amino acid residues that contacted the previously indicated species with a spacing of 0.35 Å and radii of 0.06 Å using AutodockTools [28]. Graphics and molecular analysis were performed with the UCSF Chimera software [36].

4.10. Statistic Analysis of the Data

Data shown in this manuscript are the average of experiments performed in triplicate with the standard deviation of the data. Statistical analysis of the results was performed by applying the T-student analysis to determine the statistical significance of the data * $p < 0.05$, ** $p < 0.01$, *** $p < 0.001$.

Supplementary Materials: The following supporting information can be downloaded at https://www.mdpi.com/article/10.3390/molecules28010123/s1: Figure S1: Absorbance spectra of the flavylium salts after addition to the buffer, and after incubation for 2 minutes in these conditions; Figure S2: The UV-vis spectra of the non-equilibrated form of compounds **1** and **5** after instant measurement of the spectra of the acidified solution upon addition to 100mM of potassium phosphate pH 7.0 (non-equilibrated conditions) or by incubation in this buffer for 24h (equilibrated conditions); Figure S3: Alignment of the rat Cb_5R sequence of the PDB used in this study (PDB file:1I7P) and the sequence of human soluble Cb_5R (Unitpro code: Q6BCY4). Figure S4. ^{1}H NMR spectrum (400 MHz) of compound **3** in 99:1 (*v*:*v*) CD3OD:DCl 20% in D_2O. Figure S5. ^{13}C NMR spectrum (101 MHz) of compound **3** in 99:1 (*v*:*v*) CD3OD:DCl 20% in D_2O. Figure S6. HRMS spectrum of compound **3**.

Author Contributions: Conceptualization, A.K.S.-A.; methodology, A.K.S.-A. and N.B.; validation, O.H.M.-C., L.R.-M., and S.M.C.; formal analysis, A.K.S.-A., O.H.M.-C., L.R.-M. and S.M.C.; resources, A.J.P., A.K.S.-A. and N.B.; writing—original draft preparation, A.K.S.-A.; writing—review and editing, A.K.S.-A. and N.B. All authors have read and agreed to the published version of the manuscript.

Funding: This research received no external funding.

Institutional Review Board Statement: Not applicable.

Informed Consent Statement: Not applicable.

Data Availability Statement: Data are contained within the article or supplementary material. The raw data presented in this study are available on request from the corresponding author (A.K.S.-A.).

Acknowledgments: Authors would like to acknowledge the Biochemistry Department in the Faculty of Medicine at the Universidad Autónoma de Madrid for the equipment and support for some of the required reagent purchases. This work received support from PT national funds (FCT/MCTES, Fundação para a Ciência e Tecnologia and Ministério da Ciência, Tecnologia e Ensino Superior) through the projects UIDB/50006/2020 and UIDP/50006/2020. FCT/MCTES is also acknowledged for supporting the National Portuguese NMR Network (ROTEIRO/0031/2013-PINFRA/22161/2016, co-financed by FEDER through COMPETE 2020, POCI, PORL, and FCT through PIDDAC) and for the projects UIDB/04326/2020 and PTDC/QUI-COL/32351/2017. N.B. thanks FCT for funding through the Scientific Employment Stimulus—Individual Call (Ref: CEECIND/00466/2017). We thank José Paulo da Silva for the HRMS-ESI analysis.

Conflicts of Interest: The authors declare no conflict of interest.

Sample Availability: Not applicable.

References

1. Samhan-Arias, A.K.; Gutierrez-Merino, C. Purified NADH-Cytochrome B5 Reductase Is a Novel Superoxide Anion Source Inhibited by Apocynin: Sensitivity to Nitric Oxide and Peroxynitrite. *Free Radic. Biol. Med.* **2014**, *73*, 174–189. [CrossRef] [PubMed]
2. Samhan-Arias, A.K.; Duarte, R.O.; Martín-Romero, F.J.; Moura, J.J.G.; Gutiérrez-Merino, C. Reduction of Ascorbate Free Radical by the Plasma Membrane of Synaptic Terminals from Rat Brain. *Arch. Biochem. Biophys.* **2008**, *469*, 243–254. [CrossRef]
3. Samhan-Arias, A.K.; Garcia-Bereguiain, M.A.; Gutierrez-Merino, C. Hydrogen Sulfide Is a Reversible Inhibitor of the NADH Oxidase Activity of Synaptic Plasma Membranes. *Biochem. Biophys. Res. Commun.* **2009**, *388*, 718–722. [CrossRef] [PubMed]
4. Kurian, J.R.; Chin, N.A.; Longlais, B.J.; Hayes, K.L.; Trepanier, L.A. Reductive Detoxification of Arylhydroxylamine Carcinogens by Human NADH Cytochrome B5 Reductase and Cytochrome B5. *Chem. Res. Toxicol.* **2006**, *19*, 1366–1373. [CrossRef]
5. Henderson, C.J.; McLaughlin, L.A.; Wolf, C.R. Evidence That Cytochrome B5 and Cytochrome B5 Reductase Can Act as Sole Electron Donors to the Hepatic Cytochrome P450 System. *Mol. Pharmacol.* **2013**, *83*, 1209–1217. [CrossRef] [PubMed]
6. Valério, G.N.; Gutiérrez-Merino, C.; Nogueira, F.; Moura, I.; Moura, J.J.G.; Samhan-Arias, A.K. Human Erythrocytes Exposure to Juglone Leads to an Increase of Superoxide Anion Production Associated with Cytochrome B5 Reductase Uncoupling. *Biochim. Et Biophys. Acta Bioenerg.* **2020**, *1861*, 148134. [CrossRef] [PubMed]
7. Samhan-Arias, A.K.; Almeida, R.M.; Ramos, S.; Cordas, C.M.; Moura, I.; Gutierrez-Merino, C.; Moura, J.J.G. Topography of Human Cytochrome B5/Cytochrome B5 Reductase Interacting Domain and Redox Alterations upon Complex Formation. *Biochim. Biophys. Acta Bioenerg.* **2018**, *1859*, 78–87. [CrossRef]
8. Samhan Arias, A.K.; Gutierrez-Merino, C. *Cytochrome B5 as a Pleitropic Metabolic Modular in Mammalian Cells*; Thom, R., Ed.; Protein biochemistry, synthesis, structure and cellular functions; Nova Publishers: New York, NY, USA, 2014; ISBN 978-1-63117-467-4.
9. Gutiérrez-Merino, C.; Martínez-Costa, O.H.; Monsalve, M.; Samhan-Arias, A.K. Structural Features of Cytochrome B5-Cytochrome B5 Reductase Complex Formation and Implications for the Intramolecular Dynamics of Cytochrome B5 Reductase. *Int. J. Mol. Sci.* **2021**, *23*, 118. [CrossRef]

10. Samhan-Arias, A.K.; Garcia-Bereguiain, M.A.; Martin-Romero, F.J.; Gutierrez-Merino, C. Clustering of Plasma Membrane-Bound Cytochrome B5 Reductase within "lipid Raft" Microdomains of the Neuronal Plasma Membrane. *Mol. Cell. Neurosci.* **2009**, *40*, 14–26. [CrossRef]
11. Marques-da-Silva, D.; Gutierrez-Merino, C. Caveolin-Rich Lipid Rafts of the Plasma Membrane of Mature Cerebellar Granule Neurons Are Microcompartments for Calcium/Reactive Oxygen and Nitrogen Species Cross-Talk Signaling. *Cell Calcium* **2014**, *56*, 108–123. [CrossRef]
12. Samhan-Arias, A. Biochemical and Anatomical Basis of Brain Dysfunctions Caused by Cytochrome B5 Reductase Deficiency or Dysregulation. *J. Neurol. Neuromedicine* **2016**, *1*, 61–65. [CrossRef]
13. Rahaman, M.M.; Nguyen, A.T.; Miller, M.P.; Hahn, S.A.; Sparacino-Watkins, C.; Jobbagy, S.; Carew, N.T.; Cantu-Medellin, N.; Wood, K.C.; Baty, C.J.; et al. Cytochrome B5 Reductase 3 Modulates Soluble Guanylate Cyclase Redox State and CGMP Signaling. *Circ. Res.* **2017**, *121*, 137–148. [CrossRef] [PubMed]
14. Ghimire, K.; Altmann, H.M.; Straub, A.C.; Isenberg, J.S. Nitric Oxide: What's New to NO? *Am. J. Physiol. Cell Physiol.* **2017**, *312*, C254–C262. [CrossRef] [PubMed]
15. Samhan-Arias, A.K.; Fortalezas, S.; Cordas, C.M.; Moura, I.; Moura, J.J.G.; Gutierrez-Merino, C. Cytochrome B5 Reductase Is the Component from Neuronal Synaptic Plasma Membrane Vesicles That Generates Superoxide Anion upon Stimulation by Cytochrome c. *Redox Biol.* **2018**, *15*, 109–114. [CrossRef] [PubMed]
16. Maeda, H.; Sawa, T.; Yubisui, T.; Akaike, T. Free Radical Generation from Heterocyclic Amines by Cytochrome B5 Reductase in the Presence of NADH. *Cancer Lett.* **1999**, *143*, 117–121. [CrossRef] [PubMed]
17. Maddu, N. *Diseases Related to Types of Free Radicals*; Shalaby, E., Ed.; Antioxidants; IntechOpen: London, UK, 2019. [CrossRef]
18. Gutierrez-Merino, C.; Lopez-Sanchez, C.; Lagoa, R.; Samhan-Arias, A.K.; Bueno, C.; Garcia-Martinez, V. Neuroprotective Actions of Flavonoids. *Curr. Med. Chem.* **2011**, *18*, 1195–1212. [CrossRef] [PubMed]
19. Panche, A.N.; Diwan, A.D.; Chandra, S.R. Flavonoids: An Overview. *J. Nutr. Sci.* **2016**, *5*, e47. [CrossRef]
20. Pina, F.; Melo, M.J.; Laia, C.A.T.; Parola, A.J.; Lima, J.C. Chemistry and Applications of Flavylium Compounds: A Handful of Colours. *Chem. Soc. Rev.* **2012**, *41*, 869–908. [CrossRef]
21. Verma, S.; Singh, A.; Mishra, A. Molecular Construction of NADH-Cytochrome B5 Reductase Inhibition by Flavonoids and Chemical Basis of Difference in Inhibition Potential: Molecular Dynamics Simulation Study. *J. App. Pharm. Sci.* **2012**, *2*, 33–39. [CrossRef]
22. Çelik, H.; Koşar, M. Inhibitory Effects of Dietary Flavonoids on Purified Hepatic NADH-Cytochrome B5 Reductase: Structure-Activity Relationships. *Chem. Biol. Interact.* **2012**, *197*, 103–109. [CrossRef]
23. Cruz, L.; Basílio, N.; Mateus, N.; de Freitas, V.; Pina, F. Natural and Synthetic Flavylium-Based Dyes: The Chemistry Behind the Color. *Chem. Rev.* **2022**, *122*, 1416–1481. [CrossRef] [PubMed]
24. Gavara, R.; Petrov, V.; Pina, F. Characterization of the 4′-Hydroxynaphthoflavylium Network of Chemical Reactions. *Photochem. Photobiol. Sci.* **2010**, *9*, 298–303. [CrossRef] [PubMed]
25. Basílio, N.; Petrov, V.; Pina, F. Host-Guest Complexes of Flavylium Cations and Cucurbit [7]Uril: The Influence of Flavylium Substituents on the Structure and Stability of the Complex. *ChemPlusChem* **2015**, *80*, 1779–1785. [CrossRef]
26. Calogero, G.; Sinopoli, A.; Citro, I.; Marco, G.D.; Petrov, V.; Diniz, A.M.; Parola, A.J.; Pina, F. Synthetic Analogues of Anthocyanins as Sensitizers for Dye-Sensitized Solar Cells. *Photochem. Photobiol. Sci.* **2013**, *12*, 883–894. [CrossRef] [PubMed]
27. Trott, O.; Olson, A.J. AutoDock Vina: Improving the Speed and Accuracy of Docking with a New Scoring Function, Efficient Optimization and Multithreading. *J. Comput. Chem.* **2010**, *31*, 455–461. [CrossRef]
28. Sanner, M.F. Python: A Programming Language for Software Integration and Development. *J. Mol. Graph. Model.* **1999**, *17*, 57–61.
29. Samhan-Arias, A.K.; Marques-da-Silva, D.; Yanamala, N.; Gutierrez-Merino, C. Stimulation and Clustering of Cytochrome B5 Reductase in Caveolin-Rich Lipid Microdomains Is an Early Event in Oxidative Stress-Mediated Apoptosis of Cerebellar Granule Neurons. *J. Proteom.* **2012**, *75*, 2934–2949. [CrossRef]
30. Lagoa, R.; Lopez-Sanchez, C.; Samhan-Arias, A.K.; Gañan, C.M.; Garcia-Martinez, V.; Gutierrez-Merino, C. Kaempferol Protects against Rat Striatal Degeneration Induced by 3-Nitropropionic Acid. *J. Neurochem.* **2009**, *111*, 473–487. [CrossRef]
31. Samhan-Arias, A.K.; Martín-Romero, F.J.; Gutiérrez-Merino, C. Kaempferol Blocks Oxidative Stress in Cerebellar Granule Cells and Reveals a Key Role for Reactive Oxygen Species Production at the Plasma Membrane in the Commitment to Apoptosis. *Free Radic. Biol. Med.* **2004**, *37*, 48–61. [CrossRef]
32. López-Sánchez, C.; Martín-Romero, F.J.; Sun, F.; Luis, L.; Samhan-Arias, A.K.; García-Martínez, V.; Gutiérrez-Merino, C. Blood Micromolar Concentrations of Kaempferol Afford Protection against Ischemia/Reperfusion-Induced Damage in Rat Brain. *Brain Res.* **2007**, *1182*, 123–137. [CrossRef]
33. Al Bittar, S.; Mora, N.; Loonis, M.; Dangles, O. A Simple Synthesis of 3-Deoxyanthocyanidins and Their O-Glucosides. *Tetrahedron* **2016**, *72*, 4294–4302. [CrossRef]
34. Bradford, M.M. A Rapid and Sensitive Method for the Quantitation of Microgram Quantities of Protein Utilizing the Principle of Protein-Dye Binding. *Anal. Biochem.* **1976**, *72*, 248–254. [CrossRef] [PubMed]

35. Bewley, M.C.; Marohnic, C.C.; Barber, M.J. The Structure and Biochemistry of NADH-Dependent Cytochrome B5 Reductase Are Now Consistent. *Biochemistry* **2001**, *40*, 13574–13582. [CrossRef]
36. Pettersen, E.F.; Goddard, T.D.; Huang, C.C.; Couch, G.S.; Greenblatt, D.M.; Meng, E.C.; Ferrin, T.E. UCSF Chimera—A Visualization System for Exploratory Research and Analysis. *J. Comput. Chem.* **2004**, *25*, 1605–1612. [CrossRef] [PubMed]